Systemic AAV8-Mediated Gene Therapy Drives Whole-Body Correction of Myotubular Myopathy in Dogs

David Mack, Karine Poulard, Melissa Goddard, Virginie Latournerie, Jessica Snyder, Robert Grange, Matthew Elverman, Jérôme Denard, Philippe Veron, Laurine Buscara, et al.

Molecular Therapy
Original Article

Systemic AAV8-Mediated Gene Therapy Drives Whole-Body Correction of Myotubular Myopathy in Dogs

David L. Mack,[1,2] Karine Poulard,[3,4] Melissa A. Goddard,[2] Virginie Latournerie,[3,4] Jessica M. Snyder,[5] Robert W. Grange,[6] Matthew R. Elverman,[2] Jérôme Denard,[3] Philippe Veron,[3,4] Laurine Buscara,[3,4] Christine Le Bec,[3] Jean-Yves Hogrel,[7] Annie G. Brezovec,[6] Hui Meng,[8] Lin Yang,[9] Fujun Liu,[9] Michael O'Callaghan,[10] Nikhil Gopal,[11] Valerie E. Kelly,[1] Barbara K. Smith,[12] Jennifer L. Strande,[13,14,15] Fulvio Mavilio,[3,4] Alan H. Beggs,[16] Federico Mingozzi,[3,4,17] Michael W. Lawlor,[8] Ana Buj-Bello,[3,4,18] and Martin K. Childers[1,2,18]

[1]Department of Rehabilitation Medicine, University of Washington, Seattle, WA 98104, USA; [2]Institute for Stem Cell and Regenerative Medicine, School of Medicine, University of Washington, Seattle, WA 98107, USA; [3]Genethon, 91000 Evry, France; [4]INSERM, UMR_S951, 91002 Evry, France; [5]Department of Comparative Medicine, University of Washington, Seattle, WA 98195, USA; [6]Department of Human Nutrition, Foods, and Exercise, Virginia Polytechnic Institute and State University, Blacksburg, VA 24061, USA; [7]Neuromuscular Physiology and Evaluation Lab, Institut de Myologie, 75651 Paris, France; [8]Division of Pediatric Pathology, Department of Pathology and Laboratory Medicine, Medical College of Wisconsin, Milwaukee, WI 53226, USA; [9]Department of Biomedical Engineering, University of Florida, Gainesville, FL 32611, USA; [10]Audentes Therapeutics, San Francisco, CA 94108, USA; [11]Department of Biomedical Informatics and Medical Education, University of Washington, Seattle, WA 98019, USA; [12]Department of Physical Therapy, University of Florida, Gainesville, FL 32610, USA; [13]Department of Medicine, Medical College of Wisconsin, Milwaukee, WI 53226, USA; [14]Department of Cell Biology, Neurobiology and Anatomy, Medical College of Wisconsin, Milwaukee, WI 53226, USA; [15]Cardiovascular Center, Medical College of Wisconsin, Milwaukee, WI 53226, USA; [16]The Manton Center for Orphan Disease Research, Boston Children's Hospital, Harvard Medical School, Boston, MA 02115, USA; [17]Institut de Myologie, University Pierre and Marie Curie, 75005 Paris, France

X-linked myotubular myopathy (XLMTM) results from *MTM1* gene mutations and myotubularin deficiency. Most XLMTM patients develop severe muscle weakness leading to respiratory failure and death, typically within 2 years of age. Our objective was to evaluate the efficacy and safety of systemic gene therapy in the p.N155K canine model of XLMTM by performing a dose escalation study. A recombinant adeno-associated virus serotype 8 (rAAV8) vector expressing canine myotubularin (cMTM1) under the muscle-specific desmin promoter (rAAV8-cMTM1) was administered by simple peripheral venous infusion in XLMTM dogs at 10 weeks of age, when signs of the disease are already present. A comprehensive analysis of survival, limb strength, gait, respiratory function, neurological assessment, histology, vector biodistribution, transgene expression, and immune response was performed over a 9-month study period. Results indicate that systemic gene therapy was well tolerated, prolonged lifespan, and corrected the skeletal musculature throughout the body in a dose-dependent manner, defining an efficacious dose in this large-animal model of the disease. These results support the development of gene therapy clinical trials for XLMTM.

INTRODUCTION

More than 10,000 diseases are monogenic, with a global prevalence of approximately 1 in 100.[1] Gene therapy holds the promise to treat such diseases. To date, this approach has not widely translated to treatment of monogenic disorders affecting skeletal muscle. We report here a gene therapy dose-finding study in a large-animal model of a severe monogenic muscle disease where a single systemic treatment resulted in dramatic and durable phenotype rescue. Our findings demonstrate potential application across a wide range of diseases and broadly translate to human studies.

Gene replacement therapy based on local or systemic administration of adeno-associated viral (AAV) vectors represents a potential strategy to treat inherited diseases of skeletal muscle.[2] The monogenic muscle disorder X-linked myotubular myopathy (XLMTM; OMIM 310400) is usually fatal and affects about 1 in 50,000 male births.[3] Affected infants are typically born floppy with severely weak limbs and respiratory muscles. Carrier females are occasionally symptomatic.[4]

Survival requires intensive support, often including gastrostomy feeding and mechanical ventilation; almost half of affected infants die before 18 months of age.[3] XLMTM is caused by mutations in

Received 26 September 2016; accepted 1 February 2017;
http://dx.doi.org/10.1016/j.ymthe.2017.02.004.

[18]These authors contributed equally to this work.

Correspondence: Martin K. Childers, Department of Rehabilitation Medicine, Institute for Stem Cell and Regenerative Medicine, School of Medicine, University of Washington, Seattle, WA 98107, USA.
E-mail: mkc8@uw.edu
Correspondence: Ana Buj-Bello, Genethon, INSERM, UMR_S951, 91002 Evry, France.
E-mail: abujbello@genethon.fr

Table 1. Summary Results from 9 Weeks of Age, Pre-infusion, to 17 Weeks of Age across Dosing Groups

	Mean Change				Jonckheere-Terpstra p Value for Trend	Corresponding Figure
	Saline	Low Dose	Mid Dose	High Dose		
Neurological Function						
NAS (1–10)	−3	−1	0.3	0.7	<0.01	Figures 2A–2D
Reflex score (0–4)	−0.36	0.13	0.37	0.63	<0.01	Figures 2E–2H
Limb Strength						
Forelimb extension (N•m/kg)	−0.007	0.003	0.14	0.01	<0.01	Figures 3A–3D
Forelimb flexion (N•m/kg)	−0.017	−0.004	0.055	0.052	0.01	Figures 3E–3H
Hindlimb extension (N•m/kg)	0.01	0.04	0.11	0.12	0.03	Figures 3I–3L
Hindlimb flexion (N•m/kg)	−0.014	0.021	0.085	0.007	<0.01	Figures 3M–3P
Walking Gait						
Stride velocity (cm/s)	−15.3	4.2	70.1	57.4	0.03	Figures 4A–4D
Stride length (cm)	1.6	12	27.4	26.2	<0.01	Figures 4E–4H
Respiratory Function						
Peak inspiratory flow (mL/s)	13.4	46.7	129.3	176.3	<0.01	Figures 5A–5E

the *MTM1* gene, resulting in deficiency or dysfunction of the enzyme myotubularin, a 3-phosphoinositide phosphatase.[5] The lack of myotubularin seen in XLMTM profoundly affects skeletal muscles and produces a distinctive histopathology in animal models and in patients: myofibers are smaller and organelle organization is abnormal.[6] No disease-modifying therapies are currently available for patients, but initial AAV-mediated gene transfer experiments in animal models demonstrated dramatic phenotype improvement and suggested that effective treatment might be possible for XLMTM.[7,8]

A canine model of XLMTM provided the first opportunity to test recombinant adeno-associated virus serotype 8 (rAAV8) gene transfer in a large-animal model of this disease at a volume that could be infused in clinical practice. In a previous pilot study, we reported that a locoregional infusion of an rAAV8 vector expressing canine *MTM1* (rAAV8-cMTM1) into XLMTM puppies halted progression of the disease, dramatically improved muscle strength, and markedly extended survival.[7]

The goals of the present randomized, blinded study of escalating systemic doses of rAAV8-cMTM1 in XLMTM dogs were to establish a dosing regimen using validated endpoints while assessing safety and biodistribution. We report long-term correction of skeletal muscle pathology following a single infusion of rAAV8-cMTM1 at doses compatible with clinical applications. At therapeutic doses, rAAV8-cMTM1 was well tolerated and led to expression of myotubularin protein in skeletal muscles, with repaired myofiber pathology. Most importantly, treatment with rAAV8-cMTM1 led to extended survival, recovery of neurological function, and improvements in peak airflow velocity, limb strength, and walking gait without safety concerns. These data provide strong rationale for moving therapeutic doses of rAAV8-MTM1 into clinical studies.

RESULTS

Systemic Gene Therapy Prolongs Survival and Corrects the Clinical Status of XLMTM Dogs in a Dose-Dependent Manner

We injected three escalating doses of rAAV8-cMTM1 (0.3E−14, 2E−14, and 5E−14 vg/kg) in the cephalic vein of XLMTM dogs (n = 3 per dose) at 10 weeks of age, and saline in age-matched mutant and normal littermates (n = 6 per group) as controls. We decided to include males and females in the present study. Group assignment randomization (Table S1) resulted in three males and three females in the saline-infused normal control group, one male hemizygous and five females homozygous for the *MTM1* mutation in the saline-infused XLMTM group, two males hemizygous and one female homozygous in the low-dose group, and the mid- and high-dose groups consisted of all hemizygous mutant males. The response of animals to the treatment was studied over a 9-month period (Figure S1), and summary results of outcome measures are presented in Table 1. Dosing trends, measured by the Jonckheere-Terpstra test, were calculated from the mean change in pre-infusion (9 weeks of age) to post-infusion (17 weeks of age) values. The 17-week time point was chosen because this was the only time when all saline-infused XLMTM dogs survived. Significant trends were found in every clinical and physiological readout (survival, neurological function, limb strength, gait, and respiratory function), as described below.

Prolonged Survival

Untreated, XLMTM dogs harboring a p.N155K mutation in *MTM1* become symptomatic at around 8 weeks of age, and muscular weakness progresses until approximately 5 months of age, when animals can no longer ambulate (Movie S1), necessitating humane euthanasia. Intravenous administration of rAAV8-cMTM1 at mid (2E−14 vg/kg) and high (5E−14 vg/kg) doses prolonged ambulation (Movie S2) and conferred long-term survival until the end of the 9-month observation period, whereas rAAV8-cMTM1 at low dose (0.3E−14 vg/kg)

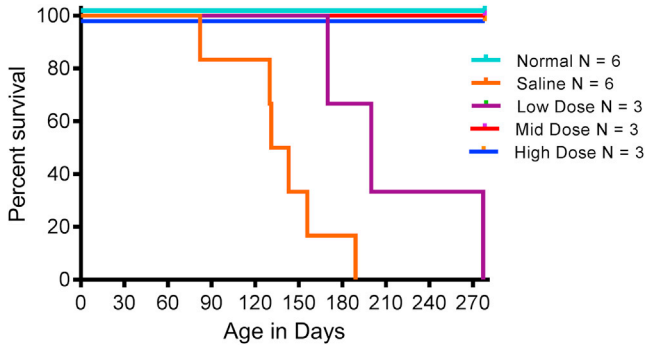

Figure 1. *MTM1* Gene Replacement with Systemic rAAV8 at Dose above 2E–14 vg/kg Markedly Extends Survival of XLMTM Dogs

Kaplan-Meier survival curves for dogs (n = 21) in one of five groups: wild-type (WT) or carrier (phenotypically normal, teal symbols, n = 6) comparison controls, or XLMTM dogs given a single venous infusion of saline (brown symbols, n = 6), 0.3E−14 rAAV8-cMTM1 (low dose, purple symbols, n = 3), 2E−14 rAAV8-cMTM1 (mid dose, red symbols, n = 3), or 5E−14 vg/kg rAAV8-cMTM1 (high dose, blue symbols, n = 3). Jonckheere-Terpstra analysis was used to test for a dosing trend across groups.

did not provide a major survival benefit over that of saline infusion, p = 0.0001 (Figure 1).

Neurological Improvement

Dogs were assessed for improvement in neurological function using a validated clinical scoring instrument developed for dogs, the neurological assessment score (NAS) (Figure 2A).[9] Results clearly demonstrated a dose-dependent effect of rAAV8-cMTM1 ($p < 0.01$) (Figures 2A–D; Table S1). Before infusion, XLMTM dogs scored slightly lower than normal controls (Figure 2C). After infusion, at the 17-week time point, NAS declined markedly in saline- and low-dose-infused dogs, whereas normal controls and XLMTM dogs given mid- or high-dose rAAV8-cMTM1 achieved comparable neurological scores (Figure 2D; Movie S3). At the end of the 9-month study, XLMTM dogs in the mid- and high-dose groups maintained neurological scores comparable with their age-matched normal controls (Figure 2B; Table S2), with dogs treated at high dose performing the best of the three dosing groups. To evaluate effects of rAAV8-cMTM1 on spinal reflexes, we recorded a clinical composite score of individual segmental reflexes (scored 0–4) for all dogs (Figure 2E). Similar to NAS, a dose-response was observed, with composite reflex scores improving quickly and dramatically between 9 and 17 weeks of age in the mid- and high-dose groups ($p < 0.01$) (Figure 2F; Table 1). At the pre-infusion time point, XLMTM dogs exhibited composite reflex scores lower than normal controls (Figure 2G). By 17 weeks, reflex function declined in saline- and low-dose-infused XLMTM dogs, and improved in dogs given mid- or high-dose rAAV8-cMTM1 (Figure 2H). At the study conclusion, XLMTM dogs receiving mid- or high-dose rAAV8-cMTM1 achieved reflex scores comparable with their age-matched controls.

Strength Improvement

In vivo isometric torque was repeatedly measured in the forelimbs and hindlimbs of anesthetized dogs from each cohort. Results (Table S3) demonstrated that saline infusion failed to halt progressive weakness, with deficiencies most notable in the muscles that pull the paw upward from the ground, mainly the extensor carpi radialis, a forelimb extensor, and the cranial tibialis, a hindlimb flexor (Figures 3A and 3M). In contrast, mid- and high-dose rAAV8-cMTM1 led to increased strength ($p < 0.01$), most notably in these same muscles (e.g., the extensor carpi radialis and cranial tibialis; Figures 3B–3D and 3N–3P, respectively).

In the forelimb (Figures 3A–3H) muscles that pull the paw upward from the ground, the forelimb extensors, a clear dose-response to rAAV8-cMTM1 was observed at 17 weeks of age ($p < 0.01$; Figure 3D). In the mid- and high-dose-infused dogs, torque values more than doubled those of saline-treated dogs. In comparison, the dose-response observed in forelimb extension was less pronounced in forelimb flexion (muscles that push the paw toward the ground, such as the flexor carpi radialis). Forelimb flexion torque in the low-dose cohort did not improve, whereas the mid- and high-dose group both improved to levels comparable with normal ($p = 0.01$; Figure 3H).

In the hindlimb, a similar dose-response trend was observed in the muscles that pull the paw upward from the ground, primarily the cranial tibialis and long digital extensor (Figures 3I–3P). In these hindlimb flexor muscles, a robust dose-response was observed at 17 weeks of age ($p < 0.01$; Figure 3P). Torque values measured in dogs given mid- and high-dose rAAV8-cMTM1 more than doubled those of saline-treated dogs. In comparison, the dose-response trend observed in hindlimb extension ($p = 0.03$; Figure 3I) was not as marked as the response observed in hindlimb flexion.

Together, the muscle performance data indicate that rAAV8-cMTM infusion at mid and high dose significantly improved torque production in forelimb and hindlimb flexion and extension of treated XLMTM dogs to values close to normal dogs.

Gait Improvement

To evaluate effects of rAAV8-cMTM1 on limb function and mobility, we evaluated gait while dogs walked over an instrumented carpet capturing spatiotemporal data.[10,11] Results show a dose-dependent effect on both gait speed ($p = 0.03$) and stride length ($p < 0.01$) (Movie S4; Table S4). At the pre-infusion assessment, XLMTM dogs demonstrated abnormally slow walking velocities with shortened stride lengths (Figure 4), consistent with our previous natural history data.[11] Over the ensuing 7 weeks, walking gait in saline-infused XLMTM dogs continued to decline; by 17 weeks of age, half of the saline-infused affected dogs grew too weak to walk repeatedly over the instrumented carpet, and only three of the six saline-infused dogs could be evaluated. In contrast, XLMTM dogs infused with rAAV8-cMTM1 showed gait improvement, but only in dogs given mid (n = 3) or high (n = 3) vector doses. These dogs achieved gait speed and stride lengths comparable with that of their normal littermates (Figures 4B and 4F; Movie S4).

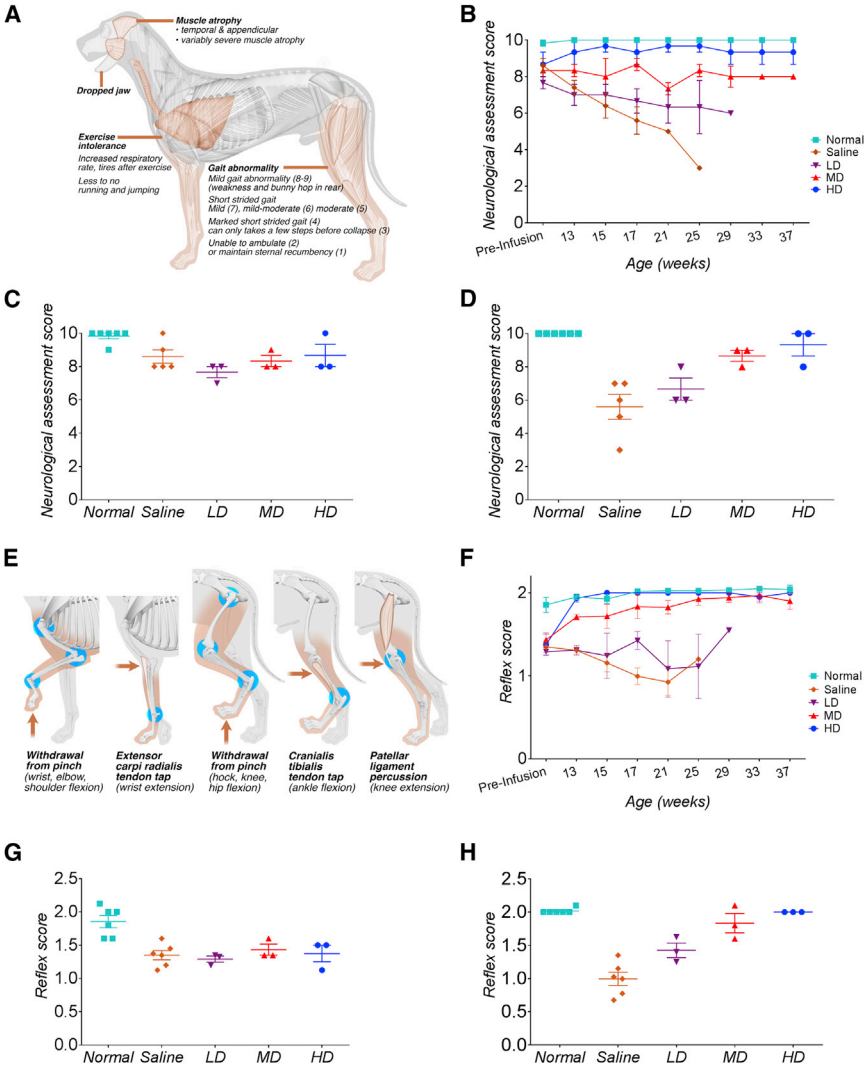

Figure 2. *MTM1* Gene Replacement with Systemic rAAV8 Halts the Progressive Decline in Global Neurological Function and Spinal Reflexes

(A) Method of the NAS. (B) NAS over time. (C and D) Group comparison of NAS before (C) and 7 weeks after (D) infusion. Trend analysis indicated a significant dose-response in NAS ($p < 0.01$). (E) Method of spinal reflex assessment. (F) Reflex scores over time. (G and H) Group comparison of reflex scores before (G) and 7 weeks after (H) infusion. Trend analysis indicated a significant dose-response in spinal reflex scores ($p < 0.01$). Jonckheere-Terpstra analysis was used to test for a dosing trend across groups. Data are presented as mean and SEM.

Intravenous Administration of rAAV8-cMTM1 Corrects XLMTM Muscle Pathology throughout the Body

To measure the extent of pathology in XLMTM dogs, we scored histological findings based on the proportion of myofibers with typical pathological features characteristic of XLMTM including small size, abnormal localization of cellular organelles, and central nucleation. Prior to treatment at 10 weeks of age, baseline disease pathology appeared comparable among all XLMTM dogs (Figure 6A; Figure S2; Table S5). Saline-treated mutant dogs developed severe muscle pathology consistent with the natural history of disease progression.[6,11] Following intravenous infusion of rAAV8-cMTM1, dogs that received the low dose failed to show improvement in disease pathology at later time points. In contrast, dogs that received either the mid or high dose of rAAV8-cMTM1 demonstrated near-complete reversal of XLMTM-related pathology, displaying essentially normal skeletal muscle histology in the majority of samples evaluated at 17 and 25 weeks of age and at euthanasia (Figures 6B–6E).

To assess whether rAAV8-cMTM1 treatment can repair the ultrastructural defects observed in myofibers, we evaluated skeletal muscles from treated and untreated dogs by electron microscopy (EM). In normal muscle, transverse-tubules are typically located with a pair of terminal cisternae (bulbous enlarged areas of the sarcoplasmic reticulum) to form an arrangement called a triad. Results (Figure 6; Table S5) indicate that a single infusion of rAAV8-cMTM1 led to normalization of disrupted sarcotubular architecture (as indicated by the number of triad structures present in the myofiber) in the mid- and high-dose-infused dogs, whereas lower numbers of triads were found in the low-dose- and saline-infused XLMTM dogs. These findings demonstrate that rAAV8-cMTM1 exerts a dose-dependent effect to repair a structural defect in the contractile apparatus associated with XLMTM.

Respiratory Function Improvement

XLMTM in children is strongly associated with neonatal hypotonia and respiratory failure;[12] an analogous phenotype is observed in XLMTM dogs.[11,13] To test for dose effects of rAAV8-cMTM1 on respiratory function, we evaluated airflow exchange in anesthetized dogs using published protocols.[11,13] We previously observed that after giving a chemical respiratory stimulant, peak inspiratory flow is lower in XLMTM compared with normal dogs. In the present study, trend analysis of peak inspiratory flow indicated a dose effect of rAAV8-cMTM1 ($p < 0.01$) (Table S4). Whereas the peak inspiratory flow declined in saline- or low-dose-infused XLMTM dogs over the 37-week study, we found that values increased to levels comparable with controls in dogs receiving mid and high doses of rAAV8-cMTM1 (Figures 5A–5D). Respiratory rate values (Figures 5E–5H) in mid- and high-dose groups achieved levels comparable with control dogs at 17 weeks, but these changes were not significantly different from pre-infusion values.

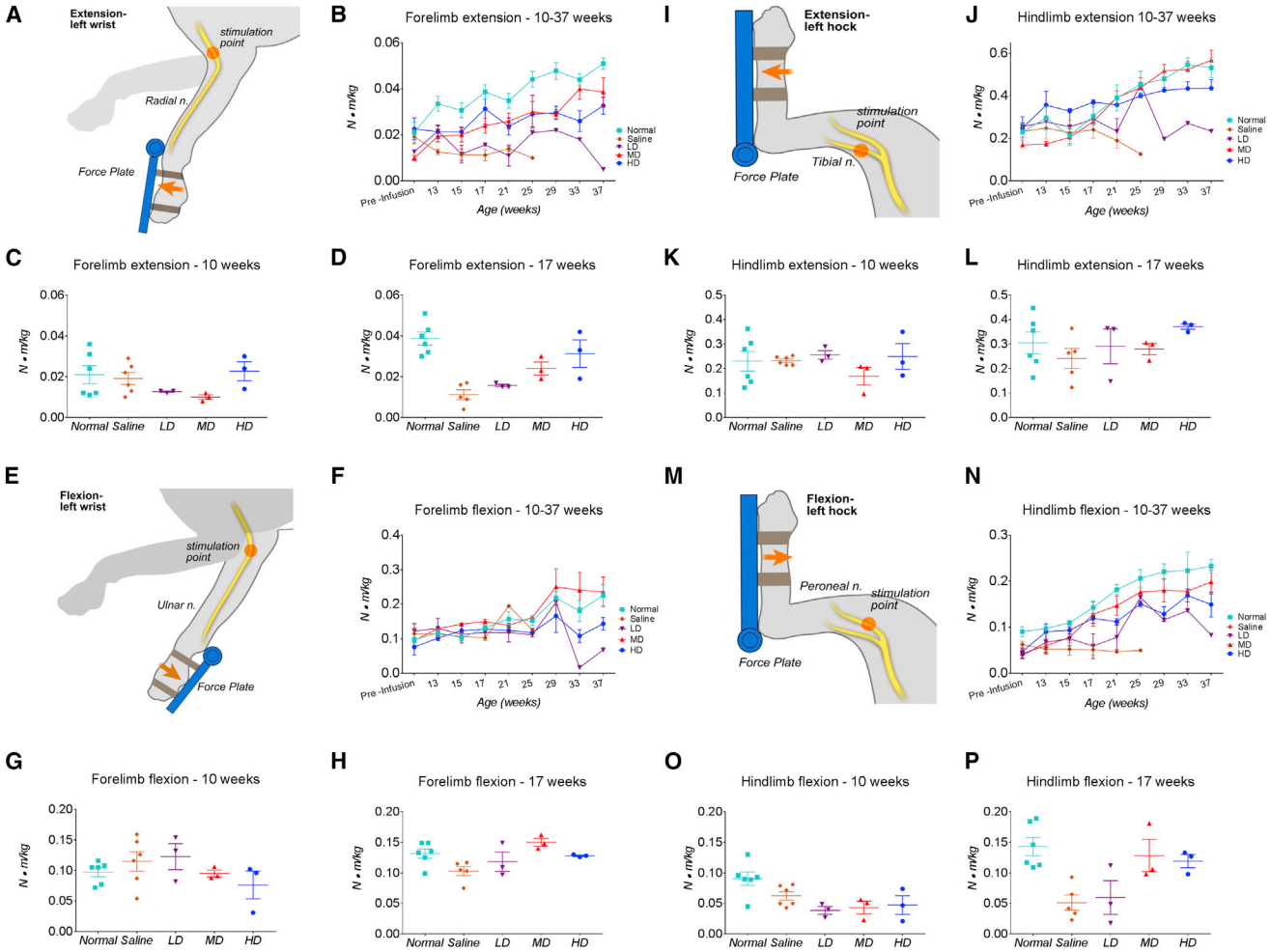

Figure 3. Progressive Loss of Limb Muscle Strength Is Ameliorated with Increasing Doses of rAAV8-cMTM1

(A) In vivo method of forelimb extensor strength testing in anesthetized dogs. A nerve stimulator delivers electrical frequencies from 1 to 150 Hz to muscles that extend, or pull, the front paw up away from the ground. A transducer captures the torque generated when the paw pushes on the force plate. (B–D) Forelimb extensor torque over time (B), before infusion (C), and 17 weeks after infusion (D). Trend analysis indicated a significant dose-response in forelimb extensor torque ($p < 0.01$). (E) In vivo method of forelimb flexor strength testing in dogs. Stimulation frequencies from 1 to 150 Hz activate muscles that push the front paw against the ground. A transducer captures the torque generated when the paw pushes on the force plate. (F–H) Forelimb flexor torque over time (F), before infusion (G), and 17 weeks after infusion (H). Trend analysis indicated a significant dose-response in forelimb flexor torque ($p = 0.01$). (I) In vivo method of hindlimb extensor strength testing. Stimulation frequencies from 1 to 110 Hz activate muscles that extend, or push, the hind paw against the ground. A transducer captures the torque generated when the paw pushes against the force plate. (J–L) Hindlimb extensor torque over time (J), before infusion (K), and 17 weeks after injection (L). Trend analysis indicated a significant dose-response in hindlimb extensor torque ($p = 0.03$). (M) In vivo method of hindlimb flexor strength testing. Stimulation frequencies from 1 to 110 Hz activate muscles that flex, or pull, the hind paw away from the ground. A transducer captures the torque generated when the paw pulls on the force plate. (N–P) Hindlimb flexor torque over time (N), before infusion (O), and 17 weeks after infusion (P). Trend analysis indicated a significant dose-response in hindlimb flexor torque ($p < 0.01$). For all figures, strength is presented as maximal isometric torque normalized to body weight (kg). The Jonckheere-Terpstra analysis was used to test for a dosing trend across groups. Data are presented as mean and SEM.

Dose-Dependent Vector Biodistribution and Transgene Expression in Tissues of Treated Dogs

We analyzed vector biodistribution in 68 tissues and organs throughout the body of XLMTM dogs. The rAAV8-cMTM1 vector transduced most tissues with the exception of brain, pancreas, and thymus (Figure 7A). In skeletal muscles, vector genomes (vg) were distributed homogenously and increased with dosage of rAAV8-cMTM1 (Figure S3; Table S6). In the mid-dose-treated cohort, vector copy number (VCN) ranged from 0.4 ± 0.1 vg/diploid genome (dg) in the diaphragm to 1.4 ± 0.4 vg/dg in the biceps femoris, whereas in dogs given high-dose rAAV8-cMTM1, VCN ranged from 1.3 ± 0.9 in the cranial tibialis to 3.2 ± 1.4 in intercostal muscles. VCN in heart and liver of high-dose-treated dogs was 2.7 ± 1.0 and 4.5 ± 1.6 vg/dg, respectively.

The vector biodistribution pattern generally correlated with transgene expression. Total MTM1 mRNA (Table S7) and myotubularin

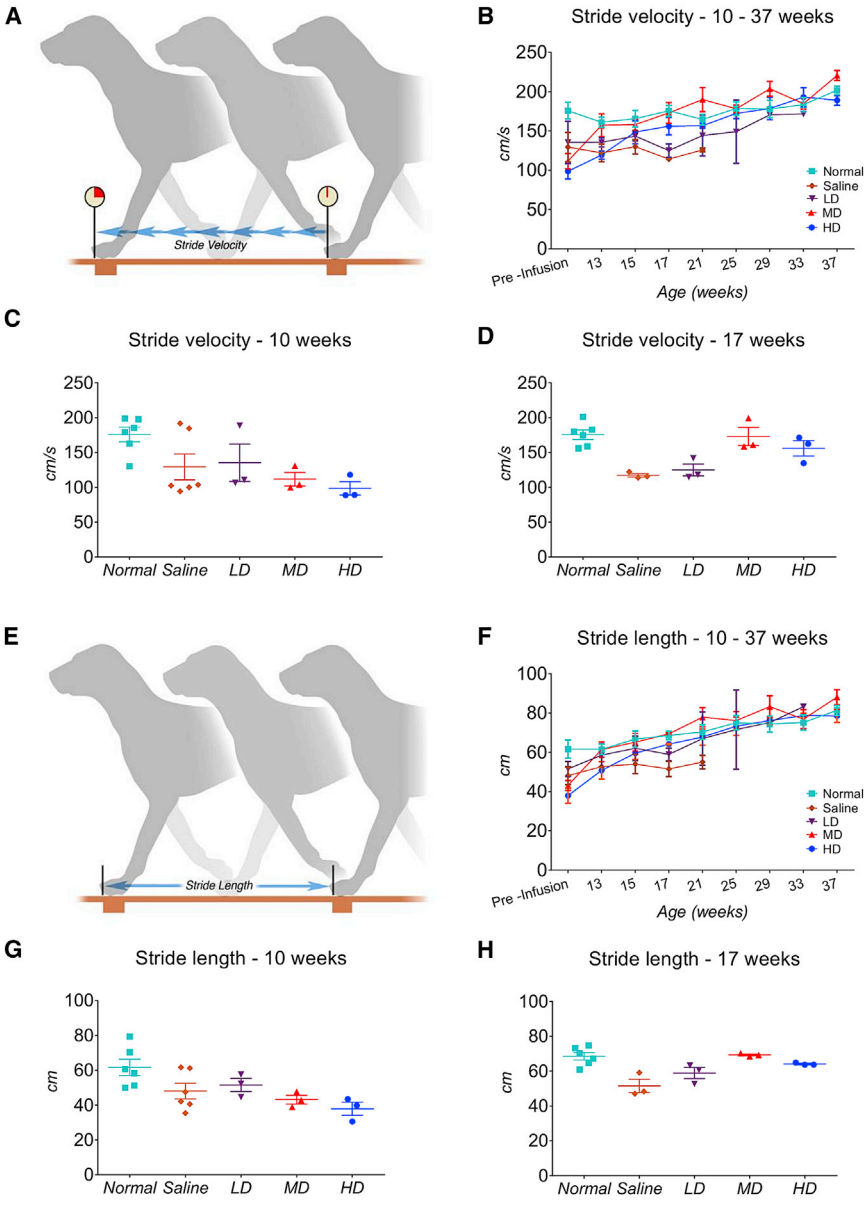

Figure 4. Walking Gait Improves with Increasing Doses of rAAV8-cMTM1

Dogs walked repeatedly over an instrumented carpet to capture spatiotemporal measures of gait. (A) Sensors imbedded in the carpet calculate walking speed. (B) Gait speed comparisons between treatment groups over the 37 weeks of study. (C) Gait speed before rAAV8-cMTM1 infusion demonstrates reduced gait speed in all XLMTM groups compared with the normal group. (D) Gait speed 17 weeks after infusion demonstrates improvement in mid- and high-dose-infused XLMTM dogs, with values comparable with normal dogs at this time point, whereas saline and low-dose dogs continue to demonstrate reduced gait speed compared with normal dogs. Trend analysis indicated a significant dose-response in gait speed ($p = 0.03$). (E) A single stride length. (F) Stride length comparisons between treatment groups over the 37 weeks of study. (G and H) Stride length among treatment groups before infusion (G) and 17 weeks after infusion (H). Trend analysis indicated a significant dose-response in stride length ($p < 0.01$). The Jonckheere-Terpstra analysis was used to test for a dosing trend across groups. Data are presented as mean and SEM.

protein levels (Table S8) were quantified in various tissues, including nine skeletal muscles, five regions of the heart (left and right ventricles, left and right atria, and papillary region), and seven other organs (liver, lung, bladder, stomach, spleen, kidney, and brain). The level of mRNA transcripts derived from the vector and the total level of MTM1 mRNA (endogenous + vector-derived) was higher in skeletal muscles and heart compared with other tissues of rAAV8-cMTM1-treated dogs, reflecting the muscle specificity of the desmin promoter. Transgenic myotubularin protein was found mostly in muscles, and its expression level increased with increasing doses of rAAV8-cMTM1, ranging from 15% of endogenous wild-type (WT) myotubularin level in the diaphragm to about 50% in other skeletal muscles of XLMTM dogs treated with the mid dose. In dogs receiving the high dose, myotubularin level reached 80% of the endogenous level in the tibialis cranialis, 220% in the intercostal muscles, and 440% in whole heart (mean range in the five cardiac regions: 260%–770%; Figures 7B and 7C; Figure S3; Table S8). These findings indicate that rAAV8-cMTM1 distributed throughout the body of XLMTM dogs in a dose-dependent manner, and the amount of myotubularin produced in skeletal muscles in the mid-dose-treated group was sufficient to correct the disease phenotype.

Safety Profile of rAAV8-cMTM1 Vector Delivery in XLMTM Dogs

Cephalic venous infusion was well tolerated without adverse events in all dogs. We found no significant changes in complete hematology counts, serum electrolytes, or kidney function and liver function parameters measured weekly following rAAV8-cMTM1 infusion. In addition, no adverse effects related to the experimental procedures were observed in dogs.

Because high overexpression of myotubularin in the heart of *Mtm1* knockout (KO) mice was reported to induce cardiac lesions,[7] we assessed potential off-target effects of rAAV8-cMTM1 on heart function using two-dimensional echocardiography with Doppler imaging (Table S9) and histology. After referencing published nomograms,[14] we estimated that an ejection fraction >60% was normal for left ventricular (LV) systolic function. Saline-infused XLMTM dogs showed normal ejection fraction at 17–18 weeks (range 62%–78%), although

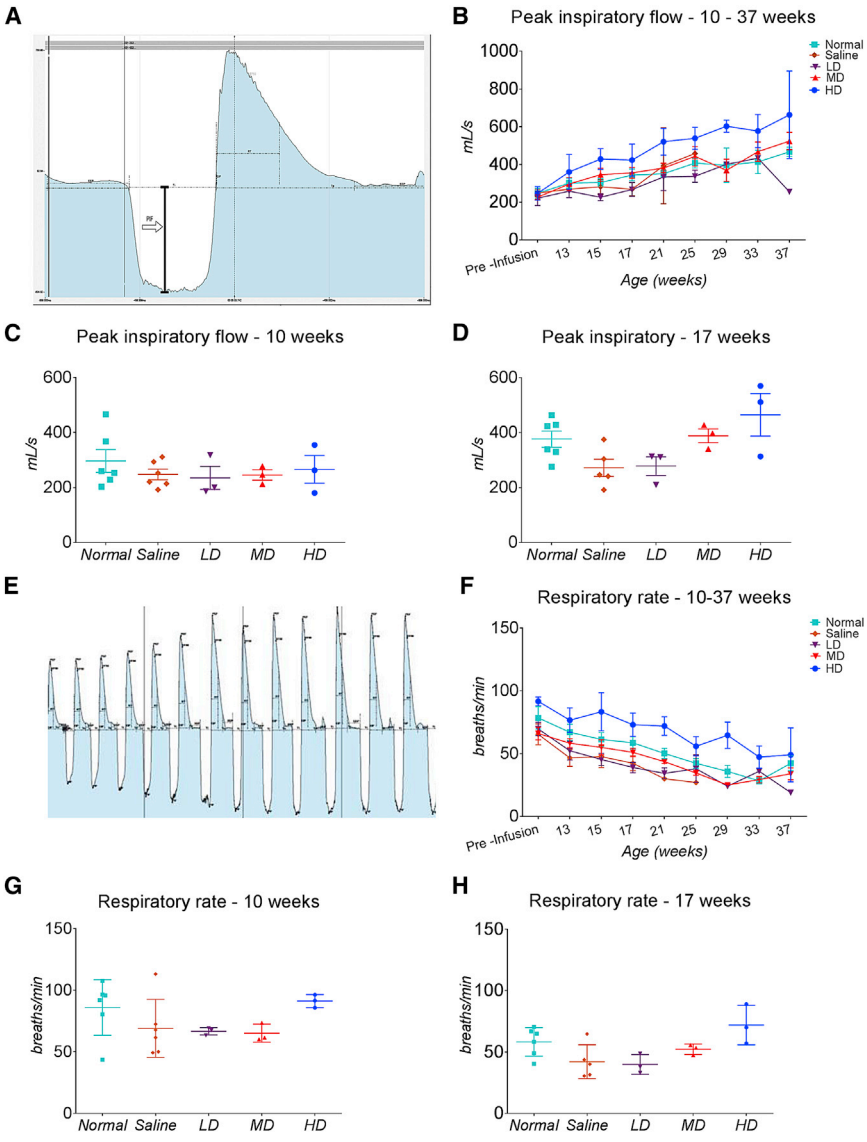

Figure 5. Peak Inspiratory Flow Improves with Increasing Doses of rAAV8-cMTM1

(A) Representative screen shot of a single breath; arrow indicates peak inspiratory flow. (B) Comparison of peak inspiratory flow in all treatment groups from 9 (pre-infusion) to 37 weeks. (C and D) Peak inspiratory flow prior to (C) and 17 weeks after (D) rAAV8-cMTM1 infusion. (E) Representative screen shot of a train of single breaths over time. (F) Comparison of respiratory rate across all treatment groups from pre-infusion up to 37 weeks. (G) Respiratory rate prior to infusion. (H) Respiratory rate at 17 weeks. Trend analysis indicated a significant dose-response in peak inspiratory flow ($p < 0.01$). The Jonckheere-Terpstra analysis was used to test for a dosing trend across groups. Data are presented as mean and SEM.

they had abnormalities in diastolic function as assessed by measuring mitral inflow velocity ratios (E/A), mitral valve (MV) annulus tissue velocity (e′), and intraventricular relaxation time (IVRT). At 17–27 weeks, the female carriers showed mild decrease in LV systolic function (52% and 57%) compared with the male controls and saline-infused XLMTM dogs (range 61%–86%). The LV systolic function in the carrier/control group normalized by 38–52 weeks (range 64%–78%). Of the dogs receiving rAAV8-cMTM1, one XLMTM dog that received low-dose rAAV8-cMTM1 also had a mild decrease in ejection fraction (54%) at 17–18 weeks, which further decreased at 27 weeks (45%) and was associated with mild diastolic dysfunction. This dog did not receive further echocardiograms. In dogs receiving either the mid- and high-dose rAAV8-cMTM1, no abnormalities of LV systolic function were detected between 17 and 27 weeks, although one dog that received mid-dose rAAV8-cMTM1 had borderline normal systolic function (59.9%) with normal diastolic function. Wall thickness was normalized to body weight in the growing dogs. Increased wall thickness of the LV septal and posterior wall was observed in two dogs (at 27 and 38 weeks) that received mid-dose rAAV8-cMTM1. The increase in wall thickness was also observed in dogs at 18 weeks that received the high-dose rAAV8-cMTM1, and the increase in septal wall thickness persisted at 27 weeks despite normalization of posterior wall thickness.

Light microscopic evaluation of heart slides taken from vehicle control, untreated control, and AAV-MTM1-treated XLMTM dogs were independently evaluated by a veterinary pathologist. Findings revealed minimal to mild infiltration of mononuclear and/or mixed inflammatory cells on the epicardium, myocardium, and/or endocardium of the heart. These findings occurred in a few control and treated animals in a non-dose-related manner and were not associated with degeneration, mineralization, loss of cardiomyocytes, and myocardial fibrosis or other cardiomyopathic changes. Similar cellular infiltrates in the heart were considered incidental, naturally occurring background changes in laboratory dogs.

Intravenous Administration of rAAV8-cMTM1 Induces No Humoral or Cytotoxic Immune Response Directed toward the Transgene Product in Mutant Dogs

We analyzed the humoral and cellular immune responses of XLMTM dogs toward the vector capsid and canine myotubularin at various time points prior to and following intravascular vector administration (Figure S4). Neutralizing antibodies (NAB) and IgG titers specific to rAAV8, and antibodies against myotubularin were measured in dog sera before and after delivery of the three doses of rAAV8-cMTM1

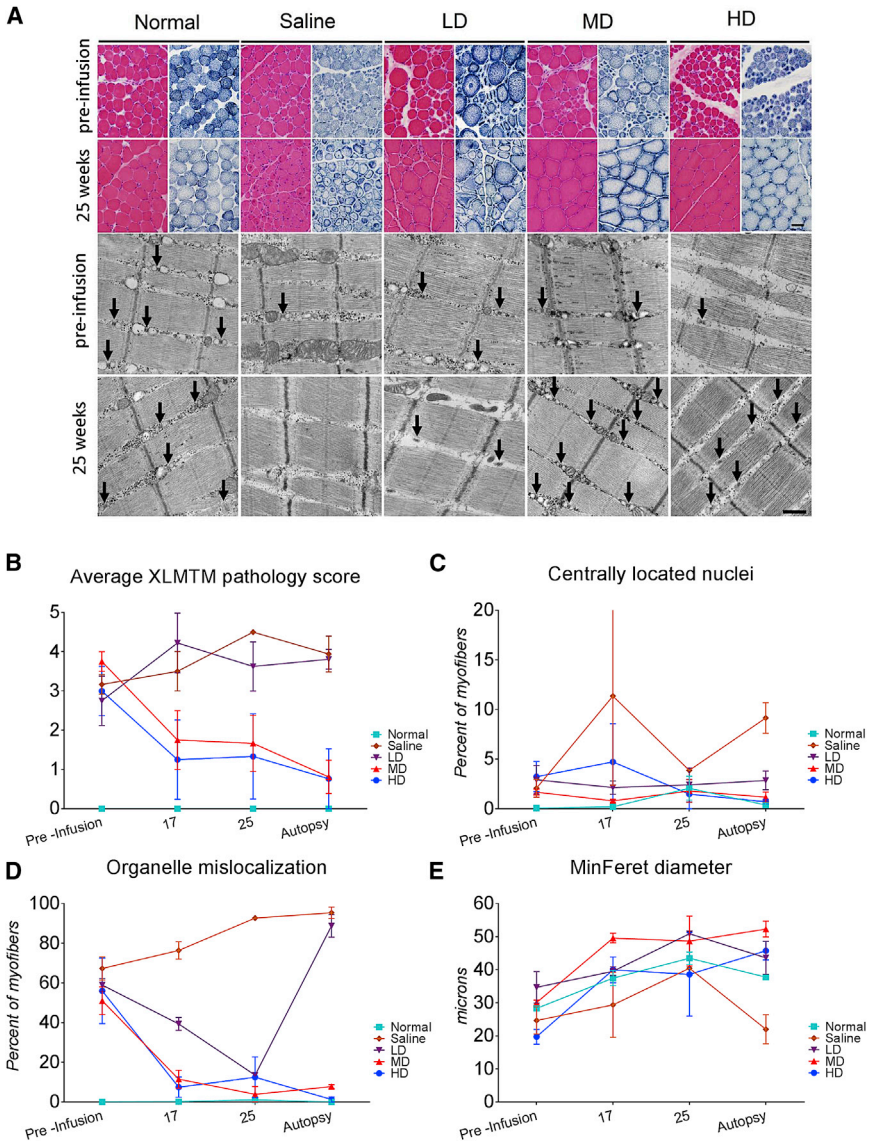

Figure 6. A Single Infusion of rAAV8-cMTM1 Can Reverse Skeletal Muscle Pathology

(A) Representative micrographs of vastus lateralis muscle samples taken from normal and XLMTM dogs at 10 weeks (pre-infusion) and at the post-infusion intervals indicated. Myofiber size and nuclear position is illustrated on H&E staining, as shown on the red-stained images. NADH staining, as shown on the blue-stained images, illustrates organelle distribution. The presence and organization of triad structures (arrows) are best illustrated on the black-and-white electron micrographs. Scale bar, 40 μm. (B–E) Histological findings were quantified to determine (B) muscle pathology scores, (C) the percentage of myofibers with centrally located nuclei, (D) the percentage of myofibers with abnormal organelle distribution, and (E) the MinFeret diameter. One-way ANOVA followed by Bonferroni's multiple comparison post-test was used to compare results between groups. Data are presented as mean and SEM.

and in the control group. NAB and IgG titers against the AAV8 capsid increased 2 weeks after vector injection and remained elevated through the end of the study in all treated animals. No clear differences in the level of antibodies were noted among dose groups. Conversely, myotubularin-specific IgG remained undetectable in all treated animals. Cell-mediated immune responses against the vector or the transgene product were tested regularly over a period of 218 days after vector administration. No T cells specific to the vector capsid or to myotubularin were detected in the blood of treated dogs.

DISCUSSION

The present study was designed to model systemic dosing of rAAV8-MTM1 gene therapy in a future clinical trial in patients. It was conducted in a large cohort of XLMTM dogs to determine the vector safety profile, measure efficacy with clinically relevant endpoints, analyze vector biodistribution, and examine immunological responses to both the vector and the transgene product across three doses. Our study demonstrates that AAV8-mediated gene therapy can effectively correct the entire skeletal musculature in a large-animal model of an inherited fatal myopathy following a single intravenous vector administration, with widespread implications for the treatment of other congenital muscle diseases.

The feasibility of MTM1 gene replacement with rAAV was previously tested in *Mtm1* KO mice by intramuscular and tail vein injections,[7,15] and then in a pilot study in XLMTM dogs by locoregional infusion of a hindlimb,[7] showing long-term benefits. The injection of a single dose of rAAV8-cMTM1 under high pressure into the saphenous vein of 9-week-old dogs resulted in the correction of the pathology in the infused hindlimb, but also in distal muscles, with an unexpected systemic effect and prolongation of lifespan.[7] This whole-body phenotypic correction varied among dogs, probably depending on the amount of vector that went into the general circulation after tourniquet release. In the present study, we tested a more clinically relevant route of administration by simple injection of rAAV8-cMTM1 into a peripheral vein, the cephalic vein of the upper limb, and performed a dose-finding study in XLMTM dogs at 10 weeks of age when pathology is well established in skeletal muscles.[11] Because of both ethical and cost considerations, we included *MTM1* mutant hemizygous male and homozygous female XLMTM dogs, and animals were randomized into the various study groups. In our colony, homozygous females present a phenotype similar to that of hemizygous males. Both male and female XLMTM dogs develop muscle weakness, gait abnormalities, and neurological

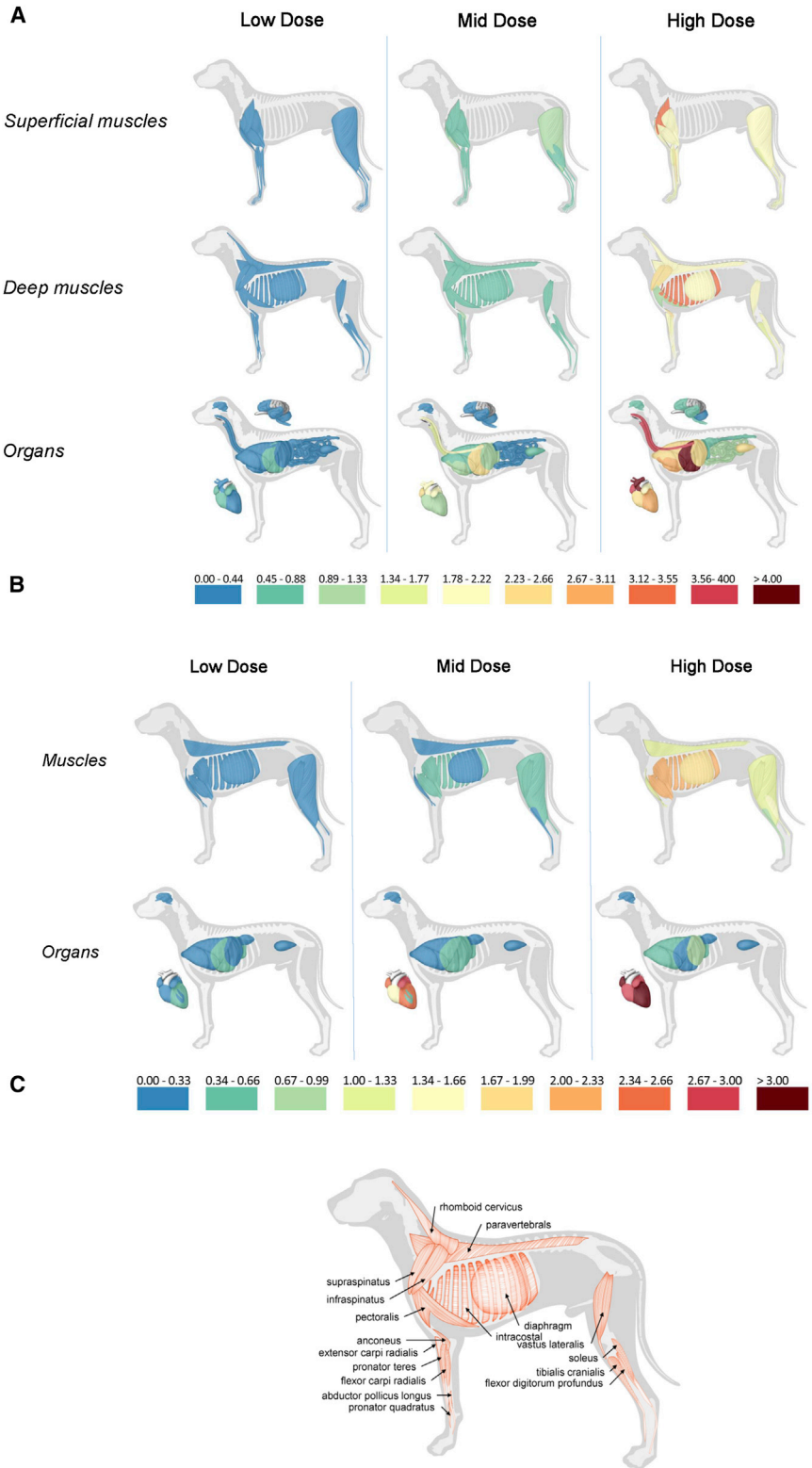

Figure 7. A Single Infusion of rAAV8-cMTM1 Yielded Whole-Body Vector Biodistribution, Leading to Myotubularin Expression that Increased with Dose

(A) Schematic depiction of canine anatomy showing a subset of muscles and organs analyzed at necropsy for the presence of rAAV8 vg. PCR-detected vg per canine dg from each muscle and organ were averaged within each treatment group, converted to a color gradient and overlaid on the dogs' anatomy. (B) Using similar methodology, we used semiquantitative western blots to measure transgenic MTM1 protein expression. Expression levels were averaged for individual muscles and organs within each treatment group and converted to a color gradient with normal endogenous levels of MTM1 protein in each tissue assigned a value ~1. (C) Key for individual muscles shown in (A) and (B).

impairment at a similar rate and progression. In the present study, randomization led to non-equal distribution with regard to sex, with female dogs more heavily represented in the saline group and only one female included in the low-dose group. Therefore, sex-related phenotype differences in the low-dose or saline groups cannot be ruled out; however, they did not confound any of the readouts in the mid- and high-dose groups because these cohorts consisted of all males.

The first major finding reported here is the dose-dependent improvement in strength to levels approaching normal following *MTM1* gene transfer. Severe weakness is the key clinical characteristic of the disease, and thus muscle strength represents the most important readout. We observed improved muscle torque performance in both forelimbs and hindlimbs of XLMTM dogs to levels comparable with normal dogs, indicating complete rescue of muscle function following mid and high dose of rAAV8-cMTM1. Some of the functional results (forelimb and hindlimb flexion torque, stride velocity, and length) indicate that the mid dose is equal to, or sometimes better, than the high-dose readouts at 17 weeks, a time when all four cohorts could be measured. However, the NAS, forelimb extension torque, hindlimb extension torque, and peak inspiratory flow values at 17 weeks indicate that 5E−14 vg/kg of vector resulted in slightly better responses. Despite these variations, statistical analyses detected positive dosing trends in the majority of functional assessments as indicated in Table 1, although a clear ceiling to the response at the mid dose cannot be confidently determined. Importantly, our study identifies systemic doses of rAAV8 (2E−14 and 5E−14 vg/kg) that led to a reversal of the disease phenotype in XLMTM dogs to a state clinically indistinguishable from normal without additional safety concerns. The rescue of XLMTM muscle function with rAAV8-cMTM1 infusion at the mid dose or above was also consistent with improved muscle reflexes and increased gait speed.

Joint movements used for gait require paired agonist and antagonist muscle groups. We did not measure dramatic changes in hindlimb extension and forelimb flexion torque in the mid- and high-dose cohorts, possibly because these muscle groups contract against a load during gait. Thus, loaded muscles in XLMTM may be able to maintain strength because of the stresses experienced, and did not improve following rAAV8 infusion as much as the improvement observed in non-loaded limb muscle groups. However, improvements in hindlimb flexion and forelimb extension would still contribute to improved gait because of improved flexion-extension symmetry at the ankle joints. Furthermore, although we did not assess knee or hip and shoulder joint muscle agonist-antagonist muscle groups, improvements in these non-studied muscle groups may have occurred following mid- and high-dose rAAV8 infusion. The best evidence to support this possibility is the near-normal gait observed in the treated dogs after mid- or high-dose rAAV8 (see Movies S1, S2, S3, and S4) that suggests better joint symmetry.

Because walking gait does not require maximal muscle torque, improvements in gait could be expected even for animals with more modest increases in maximal muscle torque. There are a number of reasons why gait analysis is complementary to (not redundant with) muscle torque measurements. Gait assessment provides a functional, behavioral measure in awake animals, while muscle torque isolates function of a given muscle (or muscle group) and is assessed in anesthetized animals. While both assessments provide slightly different information, muscle torque might be considered as an isolated measure of muscle performance, whereas gait reflects a more integrated measure of function. Similarly, respiratory function, which involves the strength of various skeletal muscles including the diaphragm, was also comparable with normal controls in the mid- and high-dose groups of treated XLMTM dogs. Furthermore, the normalized myofiber morphology and orientation of the triads suggests excitation-contraction coupling (ECC) improvement to support greater muscle torque production. Therefore, these results identify an effective threshold dose of 2E−14 vg/kg rAAV8-cMTM1 in dogs, consistently measured by separate and distinct study endpoints, which is similar to the dose (2E−14 vg/kg, transgene-specific titration) that we uniquely tested in our previous locoregional studies.[7]

We did not explore other doses below the rAAV8 mid dose (2E−14 vg/kg) or above the low dose (0.3E−14 vg/kg); thus, we cannot rule out the possibility that an intermediate dose (e.g., 1E−14 vg/kg) might result in a similar response profile. These results also suggest a potential ceiling effect of rAAV8-cMTM1, which may be related to the levels of myotubularin reached in skeletal muscles after vector transduction. The amount of transgenic myotubularin in skeletal muscles ranged from 15% to about 50% of WT endogenous levels in mid-dose-treated dogs, whereas the higher vector dose resulted in increased levels of myotubularin from 80% to 220%. Therefore, it is likely that the presence of myotubularin in muscles at lower levels than the endogenous protein is sufficient to rescue the XLMTM phenotype, as suggested in our previous studies.[7] Because the effective threshold dose of 2E−14 vg/kg could present manufacturing challenges for clinical trials, future preclinical efforts to test new vectors that can achieve similar results, but at lower doses, would be desirable. Furthermore, concerns about potential off-target effects, such as in the liver, might provide additional rationale to investigate liver detargeting alternative vectors designed by site-directed mutagenesis, such as AAV2i8, or the muscle-specific AAV2i8G9 chimera.[16,17] Alternatively, a concomitant short course of glucocorticoid therapy in patients could be used to prevent or control a potential transient hepatitis associated with systemic vector delivery, as previously demonstrated in clinical trials using high doses of rAAV8 or rAAV9.[18,19]

Intravenous delivery of rAAV8-cMTM1 led to efficient transduction of skeletal muscles, diaphragm, heart, liver, and other tissues. We observed a clear dose-dependent increase in VCN in the large panel of analyzed tissues and a homogeneous biodistribution of the vector in muscles across the body. Interestingly, the amount of rAAV8 vector in the liver of dogs was much lower compared with that reported in other species, such as mice and nonhuman primates,[20–22] and represented barely twice as much as that observed in muscles, which

indicates that differences in vector tropism exist among different animal species.[23] Although translation of body-wide gene therapy to large-animal models of a generalized myopathy has remained challenging until recently,[7] another report has demonstrated the feasibility of muscle transduction following a simple intravenous injection of a rAAV9 micro-dystrophin vector in a dog model of Duchenne muscular dystrophy (DMD).[24] In their reported study, which lasted 4 months, the vector was administrated at a comparable dose (5–6E−14 vg/kg) in two juvenile DMD dogs under immune suppression (cyclosporine and mycophenolate mofetil) prior and throughout the entire experiment. Conversely, in our study, XLMTM dogs did not require immune-suppression treatment, nor did they develop humoral and/or cellular immune responses against the transgene product or a T cell response against the vector capsid upon rAAV8-cMTM1 administration, which probably explains the long-lasting effect of gene transfer in this animal model. This difference might be because of the nature of XLMTM pathology per se, because contrary to DMD, XLMTM is not associated with either muscle inflammation or with cycles of myofiber degeneration-regeneration.[11,25] In addition, the transgene product is unlikely to be recognized as a foreign protein because untreated XLMTM dogs carry a missense mutation with a residual amount of myotubularin in tissues.[26]

Systemic administration of rAAV8-cMTM1 was well-tolerated without adverse events in treated dogs, even at high dose (5E−14 vg/kg). Complete hematology counts, serum electrolytes or kidney and liver function parameters remained within normal range in all dogs throughout the study. In the high-dose group, where cardiac myotubularin levels were 4-fold above normal, off-target effects of rAAV8-cMTM1 on heart function (ejection fraction) were not detected, even though a mild increase in left ventricle wall thickness was found. Dogs that received mid-dose (2E−14 vg/kg) rAAV8-cMTM1 had increased LV thickness, but this change occurred later than in the high-dose group. However, increase in wall thickness was also observed in non-infused carrier and WT dogs. For example, one of the female carrier dogs had LV wall thickness that increased from mild to moderately thick from 27 to 52 weeks. Similarly, one of the male control dogs had a mild LV septal wall thickness increase at 27 weeks that progressed to moderate levels at 43 weeks. Thus, mild variations in wall thickness were seen within each study group. The interpretation of echocardiographic measurements to determine chamber size, wall thickness, and LV systolic function was based on published nomograms for dogs,[14] but have not been established for this specific breed or mix background. Therefore, it is unclear whether these mild variations of LV thickness are suggestive of effects of MTM1 overexpression in the heart or represent normal variations that may be seen in growing dogs specific to this colony. Although myotubularin protein levels in heart increased in response to vector dosage, there did not appear to be any correlations with increasing dose of rAAV8-cMTM1 and increasing wall thickness. These findings in *MTM1* mutant dogs contrast with our previous observations in *Mtm1* KO mice, where comparable systemic doses of rAAV8-Mtm1 produced myotubularin expression at higher levels in heart leading to the presence of focal inflammatory infiltrates and fibrotic lesions.[7] In treated dogs, however, no such histological lesions were observed. The observed heart lesions in mice may be explained by differences in vector transduction and expression between species, similar to differences seen previously between mouse and non-human primate liver after systemic AAV administration.[27,28] These lesions were likely related to high levels of MTM1 in the heart of KO mice, because administration of vectors detargeting cardiac expression of the transgene reduced lesions in mutant mice (unpublished data). This side effect may also be specific to mice; from a translational perspective, it indicates that cardiac monitoring should be required in XLMTM patients participating in future clinical trials.

In conclusion, our results demonstrate that systemic administration of rAAV8-cMTM1 can correct the severe generalized muscle disease in myotubularin-deficient dogs, defining a threshold dose in this animal model, and support clinical trials of gene therapy in patients with XLMTM by simple vector injection into a peripheral vein.

MATERIALS AND METHODS

Experimental Animals

XLMTM Labrador/Beagle dogs harboring a p.N155K missense mutation in the *MTM1* gene were obtained from a breeding colony at the University of Washington as previously described.[10,11,13,26,29] To generate affected male and female dogs for the present study, two hemizygous mutant males were previously infused with an AAV vector expressing the myotubularin (*MTM1*) gene as described previously.[7] One year after AAV infusion, these affected males sired both hemizygous mutant male and homozygous mutant female offspring.

Animal Care

Dogs were housed in a temperature- and humidity-monitored environment, maintained between 18°C and 26°C, and 30% and 70%, respectively. An automatic lighting system provided a 12-hr diurnal cycle occasionally interrupted for study-related activities. Dogs were co- or group-housed and only separated, as necessary, for study-related procedures. Dogs were fed once to twice daily (for a total of approximately 2 cups/day). Animals were fasted as required by specific procedures (e.g., prior to blood draws for serum chemistry or procedures involving sedation or anesthesia). Fresh drinking water was provided ad libitum and was routinely analyzed for contaminants. Enrichment toys and treats were routinely supplied. In addition, trained staff exercised the animals daily.

XLMTM-affected dogs, both hemizygous males and homozygous females, show progressive clinical deterioration beginning at about 12 weeks of age. Because of difficulty in prehending and swallowing food, or getting to the food bowl and water source, some dogs were fed by hand. In general, affected XLMTM dogs remain ambulatory until about 4 months of age. Affected dogs that can maintain sternal recumbency without human aid are generally capable of moving to their food and water source, and usually do not appear to be distressed. Criteria for humane euthanasia included inability to stand

or walk, and continued weight loss with pronounced muscle wasting despite supplemental hand feeding.

Genotyping

Puppies were genotyped from DNA isolated from oral swabs. Affected hemizygous males and homozygous mutant females carrying the *MTM1* c.465C>A variant were identified using a TaqMan assay as described previously.[26] All genotypes were confirmed on two independent specimens for each dog.

Study Design

Dogs were randomized into groups based on their genotype. XLMTM dogs included mutant hemizygous males and homozygous females, and both sexes were randomized into the study cohorts. The overall flow of the experiment and handling of individual dogs are shown in Figure S3. Investigators performing assessments were blinded to the identities of animals and to their group assignments. Three doses of rAAV8-cMTM1 were evaluated: 0.3E−14, 2E−14, and 5E−14 vg/kg, denoted as low, mid, and high dose, respectively. After randomization and baseline testing, three groups of XLMTM dogs (n = 3 per group) were given a single intravenous infusion of rAAV8-cMTM1 at 10 weeks of age: a low-dose group consisted of male (n = 2) and female (n = 1) XLMTM dogs, a mid-dose group consisted of all male (n = 3) XLMTM dogs, and a high-dose group consisted of all male (n = 3) XLMTM dogs. Saline was administered in a fourth group of male (n = 1) or female (n = 5) XLMTM dogs. A fifth group of phenotypically normal (WT male [n = 3] or heterozygous female [n = 3]) littermates served as untreated controls.

Vector Production

The recombinant AAV vector, rAAV8-cMTM1, containing the canine myotubularin coding sequence (XM850116; NCBI) downstream of the human desmin promoter was produced after baculoviral double infection of insect Sf9 cells and purified from total cell culture using AVB affinity chromatography column (AVB Sepharose high performance; GE Healthcare) as previously described.[7] The titer (vg/mL) was determined from DNase-resistant particles by a qualified droplet digital real-time PCR assay. In the present study, we used primers located in the transgene (forward: 5′-GCCTCGCCCGGACTCTA-3′; reverse: 5′-CTCAGGATCGGT GACCAGAGA-3′; probe: 5′-AGGATCCAGATCTAAGC-3′ FAM-MGB), instead of primers targeting the inverted terminal repeat (ITRg) region, which was shown to significantly underestimate genome titers.[7] Capsid titers were determined by AAV8-specific capsid ELISA (Progen). The vector was formulated in lactated Ringer's solution and controlled for sterility and purity.

Administration of rAAV8-cMTM1 or Control Vehicle

Following randomization and group assignments (Figure S3A), affected XLMTM dogs were infused with a solution of rAAV8-cMTM1 diluted in sterile 1× PBS or PBS alone infused into the cephalic vein at 10 weeks of age. Three doses of rAAV8-cMTM1 were administered in units of viral vg per kilogram body weight (vg/kg); capsid particles (cp/kg) were administered according to the randomization protocol: low-dose, 0.3E−14 vg/kg; 2E−14 cp/kg; mid-dose: 2E−14 vg/kg; 9E−14 cp/kg; high-dose: 5E−14 vg/kg; 5E−15 cp/kg. The maximum infusion volume was 5 mL/kg given at a rate of 6.7 mL/min by infusion pump. Following administration, the line was flushed with 1 mL of PBS to ensure complete delivery of the test article.

Neurological Assessments

An NAS was assigned to each dog by a board-certified veterinary neurologist (J.M.S.) as previously described,[9] who was blinded to the identity of the animals. Parameters assessed included cranial nerve function, postural reactions, segmental spinal reflexes, gait stride length, ability to run and jump, and muscle atrophy. Dogs were observed for exercise intolerance or increased respiratory rate and effort following activity. The presence or absence of a dropped jaw (ability to hold the jaw in a closed position) was also noted. Following each examination, a neurological severity score was assigned on a scale of 10 to 1, with 10 indicating a normal examination and 1 indicating an inability to maintain sternal recumbency. However, predetermined humane euthanasia criteria were usually met by an NAS score of 3. Results of neurological scoring for normal controls and for some untreated XLMTM dogs have been reported.[9]

Segmental spinal reflexes assessed included the forelimb and hindlimb withdrawal, the extensor carpi radialis, the patellar, and the cranial tibial reflexes. Reflexes were graded from 0 to 4, with 0 indicating an absent response, 1 indicating a decreased response, 2 indicating a normal response, 3 indicating an increased response, and 4 indicating a clonic response. A score was assigned to each of the five reflexes, and the five reflex scores for each dog were averaged. The average reflex score for each dog was then used to create a mean reflex score (sum of average reflex score for all dogs divided by the number of dogs in the group) for the normal control group and for the XLMTM groups at each time point.

Echocardiography and Doppler Examination

Comprehensive two-dimensional (2D) and Doppler echocardiography examinations were performed in the left lateral position using commercially available ultrasound machines (Vivid q or Vivid I; General Electric) equipped with a 3SRS sector phased array transducer. All images were digitally stored for offline analysis (EchoPAC; General Electric), and measurements were performed on three consecutive cardiac cycles and averaged. All LV measurements (short-axis view) were taken from the right parasternal location by use of the 2D-guided anatomical M-mode at the level of the papillary muscles, as recommended by the American Society of Echocardiography.[30] LV end-diastolic and end-systolic diameters, and LV posterior wall and intraventricular septal wall thickness in diastole and systole were measured. LV fractional shortening (FS) and LV ejection fraction (EF) were calculated. From the apical four-chamber view, pulse-wave Doppler was used to obtain maximal early and late diastolic mitral flow velocities, and tissue Doppler imaging was obtained for the medial and lateral mitral valve annulus measurements. Echocardiography measurements were interpreted to determine whether

measurements of chamber size, wall thickness, or LV systolic function were within normal range, based on published nomograms.[14]

In Vivo Limb Strength

Contractile properties in canine hindlimb muscles were assessed in vivo, as described previously.[31,32] Contractile properties for canine forelimb muscles were measured in an analogous manner as described for dogs.[33] In brief, hindlimb torque of anesthetized dogs was measured by wrapping the foot to a pedal mounted on the shaft of a servomotor that also functioned as a force transducer. Forelimb torque was measured in a similar manner using a separate force transducer designed for the forelimb. Percutaneous nerve stimulation activated limb muscles to either pull the paw up toward the body or push the paw down toward the ground. Isometric contractions were performed over a range of stimulation frequencies to determine torque-frequency relationships.

Gait

An instrumented carpet (GAITRite Electronic Walkway; CIR Systems) was used to measure gait, as described previously.[10] A trained handler walked leashed dogs across the instrumented carpet at a self-selected speed for 5–10 trials. Testing ended immediately if the dog showed signs of fatigue. Fewer trials were collected for young puppies or for very weak animals. Data were collected and analyzed using software (GAITFour version 4.1; CIR Systems) with simultaneous video recording by a synchronized camera (Logitech) for quality control. Walks were selected based on consistency of pattern and speed, as well as body position and behavior along the carpet. Spatiotemporal measures of gait including gait speed and length were calculated, as described previously.[10]

Respiratory Function

Respiratory assessment was carried out in anesthetized dogs before and after stimulation by a centrally acting stimulant, doxapram hydrochloride (1 mg/kg), as described previously.[13] In brief, data were collected in intubated dogs using a calibrated pneumotachometer, where changes in pressure across the device determined airflow. Flow-volume loops were created by replaying experimental data through the appropriate analyzer (iox 2.8.0.13; EMKA Technologies) and capturing 10 consecutive breaths during stimulation with doxapram hydrochloride. Software (EMKA Technologies) calculated peak inspiratory flow (PIF), peak expiratory flow (PEF), inspired volume (IV), expired volume (EV), inspiratory time (TI), and expiratory time (TE).

VCN and Transgene Expression

The number of vg per dg (VCN) was quantified from 32 ng of total DNA by TaqMan real-time PCR using a LightCycler 480 (Roche). The canine β-glucuronidase gene was used for standardization. Primers used for vg amplification were: 5′-GCCTCGCCCG GACTCTA-3′ (forward), 5′-CTCAGGATCGGTGACCAGAGA-3′ (reverse), and 5′-AGGATCCAGATCTAAGC-3′ (probe). Primers and probe used for β-glucuronidase amplification were: 5′-ACGCT GATTGCTCACACCAA-3′ (forward), 5′-CCCCAGGTCTGCTTCA TAGTTG-3′ (reverse), and 5′-CCCGGCCCGTGACCTTTGTGA-3′ (probe) (Applied Biosystems).

mRNA Expression

Tissues were homogenized using MagNa Pure LC RNA Isolation Tissue Lysis Buffer (Roche), and total RNA was isolated using an automated nucleic acid extraction instrument (MagNA Pure 96 System), followed by DNase digestion to minimize genomic DNA contamination (DNA-*Free* DNA Removal Kit; Life Technologies). One hundred nanograms of total RNA was used to perform a one-step qRT-PCR using the LightCycler Multiplex RNA Virus Master kit (Roche) and specific oligonucleotides and probes in a LightCycler 480 (Roche). The 60 s ribosomal protein L32 (RPL32) was used for normalization. The sequences of the primers and probes were: vector-derived transcript: 5′-GCCTCGCCCGGACTCTA-3′ (forward), 5′-CTCAGGATCGGTGACCAGAGA-3′ (reverse), and 5′-AGGATC CAGATCTAAGC-3′ (FAM-MGB) (probe); canine MTM1 transcript: 5′-ATAAGTTTTGGACATAAGTTTGC-3′ (forward), 5′-CA TTTGCCATACACAATCAA-3′ (reverse), and 5′-CGACGCTGA CCGGTCTCCTA-3′ (FAM Tamra) (probe); and canine RLP32 transcript: 5′-TGGTTACGGGAGCAACAAGAAA-3′ (forward), 5′-GCACATCAGCAGCACTTCA-3′ (reverse), and 5′-TGCTGCCCA GTGGCTTCTGG-3′ (VIC-QSY) (probe).

Immunoblotting

Proteins were extracted from tissues using a lysis buffer containing 10 mM Tris HCl (pH 7.4), 150 mM NaCl, 1 mM EDTA, 1 mM EGTA, 2 mM Na orthovanadate, 100 mM NaF, 4 mM sodium pyrophosphate, 1% Triton X-100, 0.5% IGEPAL, and a protease inhibitor cocktail (Roche Applied Science), and analyzed by SDS-PAGE (NuPAGE Novex 4%–12% Bis-Tris gels; Invitrogen) and western blotting as previously described.[7] Membranes were probed with a polyclonal antibody against the C terminus of canine myotubularin (R1040; Genethon) and a mouse monoclonal antibody against GAPDH (MAB374; Millipore) as internal control. Detection was performed with a secondary antibody coupled to IRDye 680 (LI-COR Biotechnology) and the Odyssey infrared imaging system (LI-COR Biotechnology).

Heatmap Illustrations

For both the VCN and transgene data, the colors in the visualization (Figure 7) reflect the average value for each anatomical part in its dose category (low, mid, and high dose). Non-treated dogs were not used for any calculations or depictions. For the VCN data, this average was calculated over measurements from both sides of the dog. Furthermore, missing values were not included in the denominator when calculating the average. The nine-class spectral color scale from Color Brewer was employed to differentiate between average values for both the VCN and the transgene expression data.[34] Values that fall between given spectral scale color values are interpolated using the interpolation function built into D3.js.[35] When sorted in ascending order, data for both the VCN and transgene expression data are linear until a point where values begin to increase exponentially. To prevent the color scale from being skewed toward these high-value outliers

and preserve perceptual accuracy, we mapped the linear portion of the data to the spectral color scale and the remaining outlier values to a separate dark red color. For depiction of VCN, values ranging from 0 to 4 were mapped to the spectral color scale, which captures 92% of the data. Values greater than 4, which correspond to the remaining 8% of data, appear in a separate dark red color. For depiction of transgene expression, values ranging from 0 to 3 were mapped to the scale, which captures 95.5% of the data. Values greater than 3, which correspond to the remaining 4.5% of data, appear in a separate dark red color.

Humoral Immune Responses to the AAV8 Vector Capsid

An ELISA was used to detect IgG antibodies specific to the AAV8 capsid in serum samples collected from uninjected and rAAV8-cMTM1-treated dogs, as previously described.[36,37]

The neutralizing assay was performed as previously described[36–38] with some modifications. In brief, 96-well plates were seeded with 20,000 2V6.11 cells treated with Ponasterone (Invitrogen) for 24 hr. The next day, a recombinant AAV8-CMV-luciferase reporter vector was diluted in DMEM (Invitrogen Life Technology) and incubated with 3.16-fold serial dilutions (1:1 to 1:316,000) of heat-inactivated serum samples (at 56°C for 30 min) for 1 hr at 37°C. Subsequently, the serum-vector mixtures were added to cells plated earlier and incubated in DMEM plus 10% fetal calf serum (FCS) for 24 hr. Each sample was tested in triplicate. Cells were then washed in PBS and lysed for 5 min with Bright-Glo Luciferase Assay system (Promega). The luciferase activity was read on a luminometer. Transduction efficiency was measured as relative light units. The values are presented as percentage of transgene activity compared with transduction of an equal amount of vectors without serum pre-incubation. The neutralizing titer was determined as the serum dilution at which $\geq$50% inhibition occurred.

Humoral Immune Response to Canine MTM1 Protein

A customized ELISA assay was developed to detect IgG antibodies specific to the canine MTM1 protein in serum. In brief, an anti-canine MTM1 antibody (R1040; Genethon) was diluted in coating buffer (0.1 M carbonate buffer at pH 9.5) to a final concentration of 5.8 μg/ml. Two-fold serial dilutions (500 ng/ml to 7.8 ng/ml) of a dog reference standard (Bethyl Laboratories) were used to build a standard curve in the assay. After overnight incubation, blocking, and washing steps, plates were incubated 1 hr at 37°C with canine MTM1 protein. Serum samples were diluted (1/200 and 1/20) in blocking buffer and incubated 1 hr at 37°C; then a secondary anti-dog IgG-HRP-conjugated antibody was added to plates. Results in this assay are expressed as a concentration of antibodies specific for the canine MTM1 protein.

Cellular Immune Response to the rAAV8 Capsid and Canine MTM1 Protein

Cellular immune responses specific to the AAV8 capsid in dogs were monitored by IFN-γ enzyme-linked immunospot (ELIspot) assays as previously described.[39]

Tissue Collection

Muscle samples were collected and processed as described previously.[40] For biopsies, tissue from the vastus lateralis, gastrocnemius, biceps brachialis, and sartorius muscles were collected from normal and XLMTM dogs at 10, 18, and 25 weeks of age (unless the animal succumbed earlier to disease), and autopsy tissue collection was performed when animals required euthanasia (age range 17–27 weeks).

Histological Evaluation

Muscle histology was performed based on staining with H&E, reduced nicotinamide adenine dinucleotide (NADH), and an ATPase stain performed at pH 9.4. Slides were evaluated by a board-certified anatomic pathologist and neuropathologist (M.W.L.) with respect to the full range of possible pathologies. The extent of pathology was scored based upon the approximate percentage of myofibers displaying XLMTM pathology as described in dogs[6] (Figure S2). Scores were assigned as follows: grade 0 = no XLMTM pathology, grade 1 = XLMTM pathology in $\leq$10% of fibers, grade 2 = XLMTM pathology in 11%–30% of fibers, grade 3 = XLMTM pathology in 31%–60% of fibers, grade 4 = XLMTM pathology in 61%–80% of fibers, and grade 5 = XLMTM pathology in 81%–100% of fibers. The pathology scores of all muscles were averaged for each dog as an indication of pathology across the entire animal at a given time point. Formal quantitative studies were performed on the vastus lateralis specimens only. Myofiber size was evaluated on scanned H&E-stained slides and measured using an automated technique developed in our prior work.[41,42] The percentage of fibers with central nucleation and the percentage of fibers with organelle mislocalization were manually scored using images of slides stained with H&E or NADH, respectively. Muscle tissue (vastus lateralis) was fixed in 2.5% glutaraldehyde, processed at the Medical College of Wisconsin's EM Core Facility, and evaluated at each time point using a standard approach previously described.[7,8] Comprehensive reports of pathological findings at the light and EM level were prepared using an adaptation of the National Institute of Neurological Disorders and Stroke (NINDS) Common Data Elements muscle biopsy reporting form.[43]

Statistics

In this dose-escalation study, we used the Jonckheere-Terpstra nonparametric statistic for an alternative of increasing trend across the four dose groups (saline only, low-, mid-, and high-dose rAAV8-cMTM1) versus no increasing trend. For each subject the difference between the pre-infusion (week 9) and the post-infusion (week 17) value was calculated for each measured variable. This change score for each dog is used to calculate the trend statistic. There were six dogs in the saline group and three dogs in each of the three dosing groups. The number of animals that could be bred for this exploratory investigation limited the overall number of XLMTM dogs; therefore, the sample size was not based on statistical considerations. The p values reported are not adjusted for multiplicity of tests and should be interpreted in terms of consistency of effect. Statistical software used was the open-source R language.[44,45] One-way ANOVA

followed by Bonferroni's multiple comparison post-test was used for pathology readouts (Table S5).

Study Approval

Dogs were handled according to principles outlined in the NIH *Guide for the Care and Use of Laboratory Animals* and as approved by the University of Washington institutional animal care and use committee (IACUC).

SUPPLEMENTAL INFORMATION

Supplemental Information includes four figures, nine tables, and four movies and can be found with this article online at http://dx.doi.org/10.1016/j.ymthe.2017.02.004.

AUTHOR CONTRIBUTIONS

D.L.M., A.H.B., M.W.L., A.B.-B., and M.K.C. designed the study. D.L.M., K.P., M.A.G., V.L., J.M.S., J.D., P.V., L.B., C.L., H.M., L.Y., F.L., and J.L.S. performed the clinical and experimental work. R.W.G., M.R.E., A.G.B., M.O., N.G., V.E.K., and B.K.S. analyzed and discussed the results. D.L.M., A.B.-B., and M.K.C. wrote the manuscript with the help of J.M.S., R.W.G., M.R.E., J.-Y.H., N.G., V.E.K., B.K.S., J.L.S., F. Mavilio., A.H.B., F. Mingozzi, and M.W.L.

CONFLICTS OF INTEREST

A.B.-B., A.H.B., and M.K.C. are inventors of a patent on gene therapy for myotubular myopathy; A.H.B., M.W.L., and M.K.C. are members of the Board of Scientific and Clinical Advisors for Audentes Therapeutics; and A.B.-B. is a scientific advisor for Audentes Therapeutics. B.K.S. and M.W.L. receive research funding from Audentes Therapeutics and Solid GT. M.W.L. was recently a consultant for Sarepta Therapeutics and receives additional research funding from Solid GT.

ACKNOWLEDGMENTS

We thank Emily Troiano for assistance with genotyping the dogs. Some microscopic images were obtained using the Children's Hospital of Wisconsin Research Institute's Imaging Core Facility. EM was performed using the Medical College of Wisconsin's EM Core Facility. We thank Arthur Guilford for assistance with the manuscript; Kate Sweeney, at the University of Washington Visual Design and Production, who created the anatomical drawings found in several figures, but especially for her conceptual and artistic contributions on the VCN and transgene expression figures; Margaret Beatka in Pediatric Pathology at the Medical College of Wisconsin for graphic design; and Emma James of Audentes Therapeutics for editorial assistance. This work was supported in part by NIH grants R21 AR064503 and R01 HL115001 to M.K.C., grant K08 AR059750 to M.W.L., grant K08 HL111148 to J.L.S., grants R01AR044345 and HD075802 and MDA383249 (Muscular Dystrophy Association) to A.H.B.; the Senator Paul D Wellstone Muscular Dystrophy Cooperative Research Center, Seattle (NIH grant U54AR065139); the Muscular Dystrophy Association (M.K.C.); the Association Française contre les Myopathies (AFM-Telethon) (A.B.-B. and M.K.C.); the Myotubular Trust, UK (A.B.-B.); Where There's a Will There's a Cure (A.H.B. and M.K.C.); the Joshua Frase Foundation (A.H.B. and M.K.C.), the Peter Khuri Myopathy Research Foundation (M.K.C.); and Audentes Therapeutics (M.K.C., M.W.L., A.H.B., and A.B.-B.).

REFERENCES

1. World Health Organization. Genes and human disease. http://www.who.int/genomics/public/geneticdiseases/en/index2.html.
2. Guan, X., Goddard, M.A., Mack, D.L., and Childers, M.K. (2016). Gene therapy in monogenic congenital myopathies. Methods *99*, 91–98.
3. Jungbluth, H., Wallgren-Pettersson, C., and Laporte, J. (2008). Centronuclear (myotubular) myopathy. Orphanet J. Rare Dis. *3*, 26.
4. Savarese, M., Musumeci, O., Giugliano, T., Rubegni, A., Fiorillo, C., Fattori, F., Torella, A., Battini, R., Rodolico, C., Pugliese, A., et al. (2016). Novel findings associated with MTM1 suggest a higher number of female symptomatic carriers. Neuromuscul. Disord. *26*, 292–299.
5. Laporte, J., Blondeau, F., Buj-Bello, A., Tentler, D., Kretz, C., Dahl, N., and Mandel, J.L. (1998). Characterization of the myotubularin dual specificity phosphatase gene family from yeast to human. Hum. Mol. Genet. *7*, 1703–1712.
6. Lawlor, M.W., Beggs, A.H., Buj-Bello, A., Childers, M.K., Dowling, J.J., James, E.S., Meng, H., Moore, S.A., Prasad, S., Schoser, B., and Sewry, C.A. (2016). Skeletal muscle pathology in X-linked myotubular myopathy: review with cross-species comparisons. J. Neuropathol. Exp. Neurol. *75*, 102–110.
7. Childers, M.K., Joubert, R., Poulard, K., Moal, C., Grange, R.W., Doering, J.A., Lawlor, M.W., Rider, B.E., Jamet, T., Danièle, N., et al. (2014). Gene therapy prolongs survival and restores function in murine and canine models of myotubular myopathy. Sci. Transl. Med. *6*, 220ra10.
8. Lawlor, M.W., Armstrong, D., Viola, M.G., Widrick, J.J., Meng, H., Grange, R.W., Childers, M.K., Hsu, C.P., O'Callaghan, M., Pierson, C.R., et al. (2013). Enzyme replacement therapy rescues weakness and improves muscle pathology in mice with X-linked myotubular myopathy. Hum. Mol. Genet. *22*, 1525–1538.
9. Snyder, J.M., Meisner, A., Mack, D., Goddard, M., Coulter, I.T., Grange, R., and Childers, M.K. (2015). Validity of a neurological scoring system for canine X-linked myotubular myopathy. Hum. Gene Ther. Clin. Dev. *26*, 131–137.
10. Goddard, M.A., Burlingame, E., Beggs, A.H., Buj-Bello, A., Childers, M.K., Marsh, A.P., and Kelly, V.E. (2014). Gait characteristics in a canine model of X-linked myotubular myopathy. J. Neurol. Sci. *346*, 221–226.
11. Goddard, M.A., Mack, D.L., Czerniecki, S.M., Kelly, V.E., Snyder, J.M., Grange, R.W., Lawlor, M.W., Smith, B.K., Beggs, A.H., and Childers, M.K. (2015). Muscle pathology, limb strength, walking gait, respiratory function and neurological impairment establish disease progression in the p.N155K canine model of X-linked myotubular myopathy. Ann. Transl. Med. *3*, 262–278.
12. Herman, G.E., Finegold, M., Zhao, W., de Gouyon, B., and Metzenberg, A. (1999). Medical complications in long-term survivors with X-linked myotubular myopathy. J. Pediatr. *134*, 206–214.
13. Goddard, M.A., Mitchell, E.L., Smith, B.K., and Childers, M.K. (2012). Establishing clinical end points of respiratory function in large animals for clinical translation. Phys. Med. Rehabil. Clin. N. Am. *23*, 75–94, xi.
14. Sisson, D., and Schaeffer, D. (1991). Changes in linear dimensions of the heart, relative to body weight, as measured by M-mode echocardiography in growing dogs. Am. J. Vet. Res. *52*, 1591–1596.
15. Buj-Bello, A., Fougerousse, F., Schwab, Y., Messaddeq, N., Spehner, D., Pierson, C.R., Durand, M., Kretz, C., Danos, O., Douar, A.M., et al. (2008). AAV-mediated intramuscular delivery of myotubularin corrects the myotubular myopathy phenotype in targeted murine muscle and suggests a function in plasma membrane homeostasis. Hum. Mol. Genet. *17*, 2132–2143.
16. Shen, S., Horowitz, E.D., Troupes, A.N., Brown, S.M., Pulicherla, N., Samulski, R.J., Agbandje-McKenna, M., and Asokan, A. (2013). Engraftment of a galactose receptor footprint onto adeno-associated viral capsids improves transduction efficiency. J. Biol. Chem. *288*, 28814–28823.
17. Asokan, A., Conway, J.C., Phillips, J.L., Li, C., Hegge, J., Sinnott, R., Yadav, S., DiPrimio, N., Nam, H.J., Agbandje-McKenna, M., et al. (2010). Reengineering a receptor footprint of adeno-associated virus enables selective and systemic gene transfer to muscle. Nat. Biotechnol. *28*, 79–82.

18. Nathwani, A.C., Nienhuis, A.W., and Davidoff, A.M. (2014). Our journey to successful gene therapy for hemophilia B. Hum. Gene Ther. *25*, 923–926.

19. Nathwani, A.C., Tuddenham, E.G., Rangarajan, S., Rosales, C., McIntosh, J., Linch, D.C., Chowdary, P., Riddell, A., Pie, A.J., Harrington, C., et al. (2011). Adenovirus-associated virus vector-mediated gene transfer in hemophilia B. N. Engl. J. Med. *365*, 2357–2365.

20. Nathwani, A.C., Gray, J.T., McIntosh, J., Ng, C.Y., Zhou, J., Spence, Y., Cochrane, M., Gray, E., Tuddenham, E.G., and Davidoff, A.M. (2007). Safe and efficient transduction of the liver after peripheral vein infusion of self-complementary AAV vector results in stable therapeutic expression of human FIX in nonhuman primates. Blood *109*, 1414–1421.

21. Wang, L., Louboutin, J.P., Bell, P., Greig, J.A., Li, Y., Wu, D., and Wilson, J.M. (2011). Muscle-directed gene therapy for hemophilia B with more efficient and less immunogenic AAV vectors. J. Thromb. Haemost. *9*, 2009–2019.

22. Nietupski, J.B., Hurlbut, G.D., Ziegler, R.J., Chu, Q., Hodges, B.L., Ashe, K.M., Bree, M., Cheng, S.H., Gregory, R.J., Marshall, J., and Scheule, R.K. (2011). Systemic administration of AAV8-α-galactosidase A induces humoral tolerance in nonhuman primates despite low hepatic expression. Mol. Ther. *19*, 1999–2011.

23. Bell, P., Wang, L., Gao, G., Haskins, M.E., Tarantal, A.F., McCarter, R.J., Zhu, Y., Yu, H., and Wilson, J.M. (2011). Inverse zonation of hepatocyte transduction with AAV vectors between mice and non-human primates. Mol. Genet. Metab. *104*, 395–403.

24. Yue, Y., Pan, X., Hakim, C.H., Kodippili, K., Zhang, K., Shin, J.H., Yang, H.T., McDonald, T., and Duan, D. (2015). Safe and bodywide muscle transduction in young adult Duchenne muscular dystrophy dogs with adeno-associated virus. Hum. Mol. Genet. *24*, 5880–5890.

25. Romero, N.B. (2010). Centronuclear myopathies: a widening concept. Neuromuscul. Disord. *20*, 223–228.

26. Beggs, A.H., Böhm, J., Snead, E., Kozlowski, M., Maurer, M., Minor, K., Childers, M.K., Taylor, S.M., Hitte, C., Mickelson, J.R., et al. (2010). MTM1 mutation associated with X-linked myotubular myopathy in Labrador Retrievers. Proc. Natl. Acad. Sci. USA *107*, 14697–14702.

27. Hurlbut, G.D., Ziegler, R.J., Nietupski, J.B., Foley, J.W., Woodworth, L.A., Meyers, E., Bercury, S.D., Pande, N.N., Souza, D.W., Bree, M.P., et al. (2010). Preexisting immunity and low expression in primates highlight translational challenges for liver-directed AAV8-mediated gene therapy. Mol. Ther. *18*, 1983–1994.

28. Nathwani, A.C., Gray, J.T., Ng, C.Y.C., Zhou, J., Spence, Y., Waddington, S.N., Tuddenham, E.G., Kemball-Cook, G., McIntosh, J., Boon-Spijker, M., et al. (2006). Self-complementary adeno-associated virus vectors containing a novel liver-specific human factor IX expression cassette enable highly efficient transduction of murine and nonhuman primate liver. Blood *107*, 2653–2661.

29. Grange, R.W., Doering, J., Mitchell, E., Holder, M.N., Guan, X., Goddard, M., Tegeler, C., Beggs, A.H., and Childers, M.K. (2012). Muscle function in a canine model of X-linked myotubular myopathy. Muscle Nerve *46*, 588–591.

30. Lang, R.M., Badano, L.P., Mor-Avi, V., Afilalo, J., Armstrong, A., Ernande, L., Flachskampf, F.A., Foster, E., Goldstein, S.A., Kuznetsova, T., et al. (2015). Recommendations for cardiac chamber quantification by echocardiography in adults: an update from the American Society of Echocardiography and the European Association of Cardiovascular Imaging. Eur. Heart J. Cardiovasc. Imaging *16*, 233–270.

31. Kornegay, J.N., Bogan, D.J., Bogan, J.R., Childers, M.K., Cundiff, D.D., Petroski, G.F., and Schueler, R.O. (1999). Contraction force generated by tarsal joint flexion and extension in dogs with golden retriever muscular dystrophy. J. Neurol. Sci. *166*, 115–121.

32. Childers, M.K., Grange, R.W., and Kornegay, J.N. (2011). In vivo canine muscle function assay. J. Vis. Exp. (50), e2623.

33. Le Guiner, C., Montus, M., Servais, L., Cherel, Y., Francois, V., Thibaud, J.L., Wary, C., Matot, B., Larcher, T., Guigand, L., et al. (2014). Forelimb treatment in a large cohort of dystrophic dogs supports delivery of a recombinant AAV for exon skipping in Duchenne patients. Mol. Ther. *22*, 1923–1935.

34. Brewer, C.A. (1994). Color use guidelines for mapping and visualization. Visualization in Modern Cartography, *Volume 2* (Pergamon), pp. 123–148.

35. Bostock, M., Ogievetsky, V., and Heer, J. (2011). D^3: data-driven documents. IEEE Trans. Vis. Comput. Graph. *17*, 2301–2309.

36. Boutin, S., Monteilhet, V., Veron, P., Leborgne, C., Benveniste, O., Montus, M.F., and Masurier, C. (2010). Prevalence of serum IgG and neutralizing factors against adeno-associated virus (AAV) types 1, 2, 5, 6, 8, and 9 in the healthy population: implications for gene therapy using AAV vectors. Hum. Gene Ther. *21*, 704–712.

37. Monteilhet, V., Saheb, S., Boutin, S., Leborgne, C., Veron, P., Montus, M.F., Moullier, P., Benveniste, O., and Masurier, C. (2011). A 10 patient case report on the impact of plasmapheresis upon neutralizing factors against adeno-associated virus (AAV) types 1, 2, 6, and 8. Mol. Ther. *19*, 2084–2091.

38. Meliani, A., Leborgne, C., Triffault, S., Jeanson-Leh, L., Veron, P., and Mingozzi, F. (2015). Determination of anti-adeno-associated virus vector neutralizing antibody titer with an in vitro reporter system. Hum. Gene Ther. Methods *26*, 45–53.

39. Veron, P., Leborgne, C., Monteilhet, V., Boutin, S., Martin, S., Moullier, P., and Masurier, C. (2012). Humoral and cellular capsid-specific immune responses to adeno-associated virus type 1 in randomized healthy donors. J. Immunol. *188*, 6418–6424.

40. Meng, H., Janssen, P.M., Grange, R.W., Yang, L., Beggs, A.H., Swanson, L.C., Cossette, S.A., Frase, A., Childers, M.K., Granzier, H., et al. (2014). Tissue triage and freezing for models of skeletal muscle disease. J. Vis. Exp. (89), e51586.

41. Lawlor, M.W., Viola, M.G., Meng, H., Edelstein, R.V., Liu, F., Yan, K., Luna, E.J., Lerch-Gaggl, A., Hoffmann, R.G., Pierson, C.R., et al. (2014). Differential muscle hypertrophy is associated with satellite cell numbers and Akt pathway activation following activin type IIB receptor inhibition in Mtm1 p.R69C mice. Am. J. Pathol. *184*, 1831–1842.

42. Liu, F., Fry, C.S., Mula, J., Jackson, J.R., Lee, J.D., Peterson, C.A., and Yang, L. (2013). Automated fiber-type-specific cross-sectional area assessment and myonuclei counting in skeletal muscle. J. Appl. Physiol. *115*, 1714–1724.

43. Dastgir, J., Rutkowski, A., Alvarez, R., Cossette, S.A., Yan, K., Hoffmann, R.G., Sewry, C., Hayashi, Y.K., Goebel, H.H., Bonnemann, C., and Lawlor, M.W. (2016). Common data elements for muscle biopsy reporting. Arch. Pathol. Lab. Med. *140*, 51–65.

44. Team, R.C. (2015). A language and environment for statistical computing. R Foundation for Statistical Computing, http://www.R-project.org/.

45. Seshan, V.E. (2016). clinfun: clinical trial design and data analysis functions. https://cran.r-project.org/package=clinfun.